THE JOURNAL OF PHYSICAL CHEMISTRY C

Article

pubs.acs.org/JPCC

Study of Adsorption and Intercalation of Orange-Type Dyes into Mg−Al Layered Double Hydroxide

Ganna Darmograi, Benedicte Prelot,* Géraldine Layrac, Didier Tichit, Gaelle Martin-Gassin, Fabrice Salles, and Jerzy Zajac

Institut Charles Gerhardt de Montpellier, UMR-5253 CNRS-UM-ENSCM, C.C. 1502 Place Eugène Bataillon, Montpellier F-34095 Cedex 5, France

Supporting Information

ABSTRACT: In the context of depollution and textile wastewater treatment, the sorption-based processes are good candidates to achieve the efficient removal of such toxics substances as dyes. In the present study, the exchange−adsorption from aqueous solutions of three azoic dyes, Methyl Orange (MO), Orange II (OII), and Orange G (OG), onto Mg−Al−LDH−NO_3 layered double hydroxides (LDH, molar Mg:Al ratio of 2) was investigated through monitoring all retained and removed species in combination with direct calorimetry and X-ray diffraction measurements. Kinetic curves, determined for several initial concentrations of the three dyes, indicated that the process was fast (between 60 and 100 min) and followed the pseudo-second order model in line with the passage of the removed dye through a chemisorption stage, thus constituting the rate-limiting step. Dye adsorption isotherms (H2-type) showed some differences in the maximum adsorption quantity (5.5 mmol g^{-1}, MO; 2.7 mmol g^{-1}, OII; 1.7 mmol g^{-1}, OG), consistent with anionic exchange capacity and adsorption on the external surface, depending on the cross-sectional area of the dye species and with their hydrophobic−hydrophilic character. The uptake of sodium cations as a function of the dye type and the surface coverage ratio pointed that the counterions can either stay in solution or be adsorbed to neutralize the free $-SO_3^-$ moieties or other anionic species in the interlayer space. The cumulative enthalpy of displacement was negative in conformity with the exothermic character of the overall process. The intercalation of dye anions into the interlayer space of LDH materials led to its expansion with various distances being dependent both on the dye type and on the overall exchange balance. The latter included also the desorption of nitrates as well as the presence of carbonate species within the interlayer space, due to exchange in open systems exposed to the ambient atmosphere.

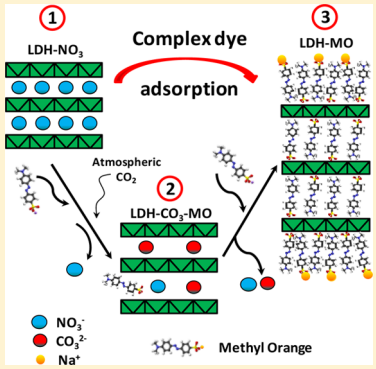

1. INTRODUCTION

The release of textile wastewater to the aquatic environment is known to cause many detrimental effects.[1] Among a wide variety of toxic substances present in the effluents generated by textile industry, dyes have the mostly diversified harmful impact on aquatic and terrestrial ecosystems, as well as on human health. Tackling and achieving the goal of "zero discharge" is a complex challenge, especially in economically weaker regions where textile is one of the most important sectors of the local economy. Chemical coagulation and flocculation is by far the mostly used technology for dyes removal, though its implementation requires significant quantities of inorganic polymers or chemical coagulants that generally involve higher cost and it also results in a high sludge production, thereby posing further handling and disposal problems. Sorption-based processes with the use of solid sorbents are good candidates for the economically and technically viable method to achieve adequate levels of dye removal at low operating cost.[2] However, the necessity of ensuring good binding affinity between the adsorbent and the adsorbing species is the principal limitation to the effectiveness of treatment technologies. The development of a new adsorbent material for efficient and economic removal of dyes from textile wastewater should be always followed by a detailed study on its working mechanism under given conditions.

The removal of anionic azo dyes from aqueous streams by layered double hydroxides (LDHs) or modified layered materials such as pillared clays is a good example of sorption-based processes proposed in the literature based on a partial comprehension of the removal mechanism and the physical factors governing it.[3−22] It is worth mentioning here that two types of adsorption systems may be considered for the study of dye retention mechanism by LDHs and it is really crucial to be sure to which system a given study is related. In a more classical case, the uptake of dye species is studied from dye-containing aqueous solutions directly by a pristine LDH sample, which includes a specific anion (e.g., NO_3^-, CO_3^{2-}, OH^-, Cl^-) compensating the positive charge of the LDH layers. In the other case referred to as "reconstruction procedure",[23] the starting LDH structure is calcined to obtain a mixed oxide

Received: June 9, 2015
Revised: September 18, 2015
Published: September 22, 2015

DOI: 10.1021/acs.jpcc.5b05510
J. Phys. Chem. C 2015, 119, 23388−23397

intermediate and the latter, in turn, is immersed in an aqueous solution containing a dye solute at a given concentration. It is usually claimed that, in the presence of water and dye anionic species, the mixed oxide intermediate is reversibly transformed back into the LDH structure, in line with the so-called "memory effect". Therefore, further description of the state-of-the-art is made by referring either to "uncalcined" (i.e., pristine) or "calcined" (i.e., reconstructed) LDH samples.

Among various reports dealing with uncalcined samples, Costantino et al. considered the intercalation of Methyl Orange (MO^-) anions into the hydrotalcite-like compound $Zn_{0.67}Al_{0.33}(OH)_2Cl_{0.33}\cdot 0.6H_2O$ via ion exchange with the pristine chloride ions up to the saturation state corresponding to 94% of the overall anionic exchange capacity (AEC) of the host.[3] X-ray diffraction (XRD) patterns recorded on uncalcined LDH samples with increasing dye uptake evidenced a stepwise increment of the interlayer spacing from 0.774 nm (the pure Cl^- phase) to 2.42 nm (the pure MO^- phase). For MO^- uptake quantities smaller than 4% of AEC, the ion exchange pathway was restricted only to the external surface of the microcrystals. The two phases containing Cl^- and MO^- were postulated to coexist in the intermediate samples up to 70% of AEC, where the Cl^- phase was completely transformed into the pure MO^- one. Further retention was regarded as solubilization of MO^- ion in the already formed phase. The computer-aided molecular modeling of the Zn−Al hydrotalcite-like layered structure with some intercalated MO anions, undertaken on the basis of the chemical composition and interlayer distance of the composite, indicated the monolayer packing of dye anions in perpendicular orientation with respect to the layer plane (their charged SO_3^- moieties in a "flip-flop" arrangement interacting with the positively charged sites). In another paper,[10] the distance of interlayer spacing in Ca−Al−LDH was shown to increase to 2.45 nm upon MO intercalation by exchange, which was regarded as reflecting a tilted orientation of the intercalated MO^- species with an angle of 49°. The intercalation of MO^- species via anionic exchange with NO_3^- counterions among the layers of the host Mg-, Ni-, and Zn-containing LDHs was monitored by UV−vis absorption spectroscopy and XRD.[6] The interlayer spacing was proven to be expanded following a two-phase transition mechanism. The maximum exchange ratio equal to 100% of the AEC was obtained only for Mg−Al−LDH, whereas it was limited to about 90% in the case of Ni− and Zn−Al−LDH. This discrepancy was rationalized by referring to a limited diffusion of MO due to a larger crystalline size of the last two LDH particles. Besides the chemisorbed MO^- ions, the compensating interlayer anions were represented mostly by OH^- and by CO_3^{2-} coming from air. Several authors applied the Langmuir, Freundlich, Temkin, or Redlich−Peterson equation to fit the experimental adsorption isotherms of MO retained by various LDHs containing either nitrate or carbonate counterions.[12−14] The kinetics of MO^- retention by LDH materials was intensely studied and often analyzed by using pseudo-first-order, pseudo-second-order, Elovich, intraparticle diffusion, and Boyd models.[5,12−14] The pseudo-second-order model provided the best fit of kinetic data in most cases, and the adsorption equilibrium, at different initial concentrations of MO, was obtained after 2 h at the most.

In the second group of papers focusing on the reconstruction and "memory effect" procedures, Zhang et al. demonstrated, on the basis of XRD and FT-IR studies, the successful intercalation of MO^- anions into calcined calcium−aluminum layered double hydroxides (Ca−Al−LDHs) in the form of inter-penetrating bilayers, paralleled by the expansion of the basal spacing of Ca−Al−LDH to 2.48 nm.[8] The results of powder XRD, FTIR, UV−vis, as well as ^{27}Al and ^{13}C CP/MAS NMR studies were also exploited by Laguna et al. to show that MO species adsorbed onto calcined Mg−Al−LDH (with a Mg:Al atomic ratio of 3) to achieve a MO content of *c.a.* 6 wt % could not be incorporated in the interlayer space, but rather on the external surface of the LDH crystals.[19] The interlayer space was postulated to be occupied by hydroxyl and carbonate anions not eliminated in the calcination stage. The possibility of intercalation of MO^- ions in flat configuration within the interlayer space of Zn−Al−LDH (with a Zn:Al molar ratio of 3) was inferred from XRD, inductively coupled plasma (ICP) emission spectroscopy, and TG-DTA measurements.[4] Taking advantage of such fitting procedures, the MO adsorption was regarded as a spontaneous (negative Gibbs free energy) and endothermic (positive enthalpy of adsorption) phenomenon.

Contrary to numerous papers dealing with the removal of Methyl Orange from aqueous solutions by LDH materials, only a few reports were published on the mechanism of adsorption of Orange II (OII) and Orange G (OG).[16−18] Bouhent et al. carried out an extended study on the adsorption of OII onto Mg−Al-LDH with the aid of powder XRD, FT-IR, UV−vis, TGA-DTA techniques.[16] They showed that OII^- anions were first adsorbed on the external surface and then intercalated within the interlayer space via ion exchange with the pristine NO_3^- counterions. The endothermic character of the adsorption phenomenon was deduced when fitting the experimental adsorption isotherms with the Langmuir model. The adsorption of OG onto Mg−Fe−LDH and Mg−Al−LDH was also investigated with the use of similar characterization methods.[17,18] The kinetic data fitted well the pseudo-second-order model and the thermodynamic consideration based on the Langmuir isotherm equation indicated that the sorption process was endothermic in nature.[17] The intercalation of OG anions into the Mg−Al−LDH interlayer space, initially containing CO_3^{2-} ions, was demonstrated to induce an increase in the basal spacing from 0.77 to 1.77 nm.[18] There were also previous studies reporting exothermic effects of sorption of dyes onto lamellar materials.[24] However, they did not describe the exchange of ionized species in pure intercalated layered anionic clays, but rather sorption on clay materials, sometimes as mixtures with other inorganic compounds.

The objective of this study was to shed more light on the mechanism of individual adsorption of three azo dyes, that is, methyl Orange, Orange II, and Orange G, from aqueous solutions onto the same pristine Mg−Al−LDH−NO_3 (molar Mg:Al ratio of 2). The equilibrium and kinetic aspects of the phenomenon in open systems exposed to the ambient atmosphere were examined in view of its potential uses in environmental remediation. Unlike previous papers that have reported on the subject, special attention was paid to the balance of various species involved in the ion exchange. The intercalation of dye anions was followed by XRD in a large 2θ range from 2° to 30°, which allowed a correct assignment of diffraction peaks. Direct calorimetry measurements of the enthalpy change accompanying the dye retention by LDH were carried out to demonstrate the exothermic character of the overall mechanism, at variance with the current state-of-the-art.

2. EXPERIMENTAL SECTION

2.1. Materials and Synthesis. The Mg−Al−LDH was prepared by coprecipitation method at constant pH (≈10). A

DOI: 10.1021/acs.jpcc.5b05510
J. Phys. Chem. C 2015, 119, 23388−23397

Table 1. Chemical Composition and Proposed Formula of Mg−Al−LDH−NO_3 as Inferred from the Elemental Analysis (The Element Contents Are Given in wt %)

Mg	Al	N	C	chemical formula	AEC (meq g^{-1})
15.85	8.78	3.81	0.32	$[Mg_{0.67}Al_{0.33}(OH)_2](CO_3)_{0.027}\cdot(NO_3)_{0.276}\cdot 1.32H_2O$	3.25

volume of 300 mL of aqueous solution containing 30.76 g of $Mg(NO_3)_2\cdot 6H_2O$ (Sigma-Aldrich) and 22.5 g of $Al(NO_3)_3\cdot 9H_2O$ (Sigma-Aldrich) was delivered by peristaltic pump into a beaker and the pH was maintained constant at pH = 10 by addition of NaOH (2 mol L^{-1}) with pH-STAT Titrino (Metrohm). After complete precipitation, the suspension was refluxed at 80 °C for 17 h, and then the gel was separated by centrifugation and thoroughly washed three times with deionized water (Na < 100 ppm). Finally, the product was dried overnight at 80 °C.

According to Table 1, the molar Mg:Al ratio was equal to 2 and the material achieved contained nitrate anions as the main interlayer compensator of the positive layer charge. Therefore, this sample was further referred to as Mg−Al−LDH−NO_3.

The SEM micrographs (see the Supporting Information) evidenced well-defined layered platelets. The appearance below 35° 2θ of three symmetric and intense peaks in the XRD pattern (see Figure S1 in the Supporting Information) corresponding to the (003), (006), and (009) harmonic reflections and above 35° 2θ of broad and asymmetric (012), (015), (110) peaks were in agreement with a well crystallized LDH exhibiting a hexagonal lattice with $R\bar{3}m$ rhombohedral symmetry. The values of the lattice parameter c = 2.67 nm and the basal spacing d_{003} = 0.89 nm agreed well with those previously reported in literature for Mg−Al−LDH−NO_3.[16,25,26] The interlayer spacing of 0.41 nm was found to be consistent with the diameter of nitrate anion (i.e., 0.40 nm[27]).

Methyl Orange, Orange II (Acid Orange 7), and Orange G (Acid Orange 10), purchased from Sigma-Aldrich, were designated MO, OII, and OG, respectively. All dyes had high purity > 99%, and they were used without any further purification. The maximum absorption (λ_{max}) in the UV−vis spectra was obtained at a wavelength of 466 nm, MO; 483 nm, OII; and 480 nm, OG. The structural formulas of the three dye anions together with their 2D molecular sizes are given in Figure 1. The estimated molecular sizes in two dimensions of the dyes were calculated with ChemDraw 3D 5.0 software package.

2.2. Characterization. The LDH morphology was observed by using a scanning electron microscope (SEM) Hitachi S-4800. The percentages of Mg and Al in the as-synthesized LDH sample were determined using energy-dispersive X-ray analysis with a Quanta 200 FEG Electron Microscopy spectrometer. The C, N, and O contents were obtained by means of CHNS-O elemental analysis (Flash EA 1112). X-ray diffraction patterns of the pristine sample were recorded with a X'Pert diffractometer over the 2θ range from 3° to 70° under the Cu Kα radiation (λ = 1.5418 Å) and nickel filter. In the case of LDH samples containing different amounts of retained dye species, the XRD patterns were collected at a scan rate of 0.003 deg min^{-1} in the 2θ range from 2° to 30° at 30 mA, 45 kV, using incident beam mask 10 mm, and zero background sample holder.

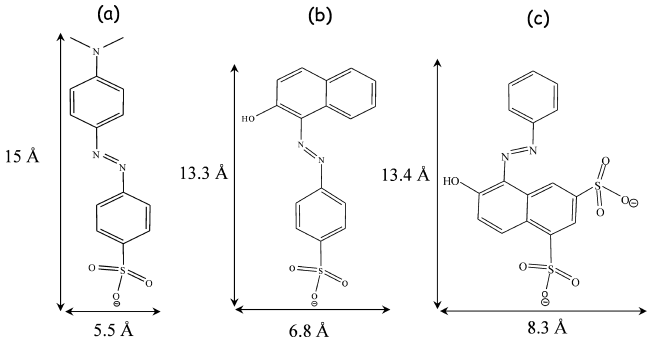

Figure 1. Structural formulas of MO (a), OII (b), and OG (c) and their 2D molecular sizes, as estimated with the aid of ChemDraw 3D 5.0 software package.

2.3. Adsorption Experiments. Classical batch adsorption studies were carried out to evaluate the retention properties of Mg−Al−LDH−NO_3. For this purpose, a LDH sample (2.5 mg) was poured into a 30 mL Nalgene tube containing 10 mL of dye solution at a given concentration. The initial concentration of dyes varied from 0.02 to 5 mmol L^{-1} for MO and OII; from 0.02 to 3 mmol L^{-1} for OG molecule. The pH of each suspension was carefully checked before and after the attainment of adsorption equilibrium. The tubes were stirred overnight at 298 K. The separation of solid phase from the supernatant liquid was achieved by centrifugating at 10 000 rpm for 12 min. The supernatant was then analyzed by using a V-670 UV−vis spectrophotometer (wavelength range 350−550 nm) to determine the equilibrium concentration of dye, C_{eq}. The amount adsorbed, Q_{ads}, was calculated as follows

$$Q_{ads} = \frac{V_0(C_i - C_{eq})}{m_s}$$

C_i is the initial dye concentration in the tube, V_0 is the initial solution volume, and m_s denotes the mass of the adsorbent. The supernatant was also analyzed with the aid of ionic chromatography analyzer (Shimadzu HPLC) equipped with a CDD-6A conductivity detector operating at 313 K (Shim-pack IC-A1 column, 2 mmol L^{-1} potassium hydrogen phthalate at pH 4.2 as the mobile phase) so as to study the amount of nitrate anions released from the LDH sample during dye adsorption. The presence of sodium counterions in the supernatant was also evaluated by the same technique (Shim-pack IC-C1 column, 5 mmol L^{-1} nitric acid as the mobile phase). The HPLC operating conditions were kept the same in both cases: flow rate of 1.5 mL min^{-1}, injection volume of 45 μL, and column temperature of 40 °C. The repeatability and experimental uncertainties of the adsorption measurements were carefully evaluated, and results are detailed in Supporting Information, section S2.

2.4. Kinetic Study. Sorption kinetics was studied by using experimental procedures similar to those described in the previous paragraph. The quantities of dye adsorption were determined at different time intervals. Three common kinetics models were subsequently applied to fit the experimental data: Lagergren-pseudo-first order,[28] pseudo-second order,[29] and Weber's intraparticle diffusion[30] one. The related analytical expressions are reported in the Supporting Information.

DOI: 10.1021/acs.jpcc.5b05510
J. Phys. Chem. C 2015, 119, 23388−23397

2.5. Calorimetry Measurements. A differential TAM III microcalorimeter was used to measure the enthalpy changes accompanying the removal of dye species from aqueous solutions by Mg−Al−LDH−NO_3. To achieve a higher sensitivity on longer time scale, the calorimeter was run in a heat flow mode. The operating procedures and data processing are detailed elsewhere.[31] Taking advantage of the oil bath system, the temperature was kept constant within ±0.0001 °C and the isothermal heat flow was measured at 25 °C. Prior to each calorimetric run, a sample of about 1−2 mg of LDH powder was introduced into the calorimetric cell initially containing 0.8 mL of deionized water. Only the same volume of deionized water was put in the reference cell. Then, both cells were placed inside the microcalorimeter and the thermal equilibrium was reached after 2 h. The injection system was equipped with a syringe filled with the appropriate stock solution of a given dye: 8.5 mmol L^{-1}, MO; 14 mmol L^{-1}, OII; 12 mmol L^{-1}, OG. Successive injections of the 10 μL aliquots of a given stock solution during 10 s resulted in an electric signal directly fed into a computer; the digitized signal representing the related thermal peaks was recorded with an equilibration time of 90 min applied between 2 injections. Integration of the areas under the thermal peaks was performed and the resulting enthalpy values were related to the mass of LDH in the cell. Similar procedures were applied to evaluate the effects of dilution and to correct the enthalpy values accordingly.[31] The repeatability of the enthalpy measurement, including the data processing step to determine the cumulative enthalpy of displacement, was within 6%, MO; 17%, OII; 4%, OG, respectively, nevertheless, the same trends in the enthalpy of displacement with the amount of dye uptaken were recorded in two separate runs.

2.6. XRD Study of the Dye-Loaded LDH Samples. Several LDH samples loaded with increasing amounts of dye were analyzed by XRD. For this purpose, 5 mg of LDH was dispersed in 20 mL of dye solution at known initial concentration. The supernatant solution was analyzed after having attained the sorption equilibrium and the corresponding dye equilibrium concentration and amount adsorbed were determined. The dye-loaded solid samples were dried at 100 °C for 1−2 h and then analyzed with the previously described XRD equipment.

3. RESULTS AND DISCUSSION

The evolution of the dye adsorption phenomena as a function of the equilibration time for the three dye species is shown in Figure S2 in the Supporting Information. In the case of MO and OG, the kinetic curves were measured for three dye initial concentrations, chosen in a way to represent the following physical situations: (i) total dye adsorption leaving a negligible quantity of the solute in the supernatant solution, (ii) adsorption system in the intermediate adsorption range, and (iii) adsorption system corresponding to the plateau saturation region. It can be clearly seen that the initial rates of MO adsorption are relatively rapid and the states near to equilibrium are reached within 60 min. It should be noted that all nitrate counterions have been already displaced from the LDH interlayer space at the end of this stage (HPLC results not shown here). Then the adsorption phenomenon proceeds at a slower rate and the final equilibrium is totally attained after 200 min. The main hypothesis at this stage is to ascribe this decrease in the MO adsorption kinetics to the removal of carbonates from LDH; the dye species need more time to replace the carbonate anions which originate from strong interactions between CO_2 molecules and the strongest basic sites in the LDHs structure, and thus it takes more time to attain the adsorption equilibrium. For OG, the adsorption equilibrium is reached after 100 min and only one step can be observed in the kinetic behavior. In the case of OII, the adsorption equilibrium is reached within the first 60 min.

Three kinetic models were used to fit the kinetic data reported in Figures S3 and S4. The resulting best-fit values of kinetic parameters have been collected in Table S1 in the Supporting Information. The highest goodness-of-fit is obtained with the pseudo-second-order model (see Figure 2)

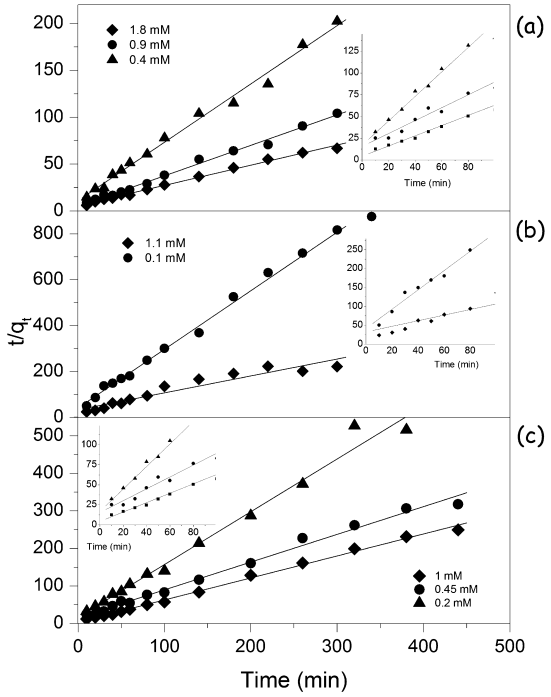

Figure 2. Pseudo-second-order kinetics model of MO (a), OII (b), and OG (c) adsorption onto Mg−Al−LDH−NO_3 for different initial concentrations.

in accordance with the literature of the subject.[13,14] This means that the dye removal passes through a chemisorption stage, which constitutes the rate-limiting process. For the sorption of MO, the rate constant k_2 obtained for the pseudo-second-order kinetic model (see kinetic equations in the Supporting Information) decreases from 0.035 to 0.008 mmol g^{-1} min^{-1} with increasing initial dye concentration.

This effect can be attributed to the increased competition for the surface active sites at higher MO concentrations.[32] It is interesting to notice that the kinetic plots following the Weber's intraparticle diffusion model do not pass through the origin. This means that the interparticule diffusion is the rate-controlling step.[33,34]

The equilibrium isotherms for the three dye molecules adsorbed onto Mg−Al−LDH−NO_3 are presented in Figure 3. For all Orange-type dyes, the amount adsorbed increases with increasing the equilibrium dye concentration. The quasi-vertical portions at very low initial concentrations reveal the high affinity of the LDH host toward the three dye species. The adsorption isotherms correspond to the H2-type according to the Giles classification.[35] The amount adsorbed levels off in the plateau region and it is approximately equal to 5.5 mmol g^{-1},

DOI: 10.1021/acs.jpcc.5b05510
J. Phys. Chem. C 2015, 119, 23388−23397

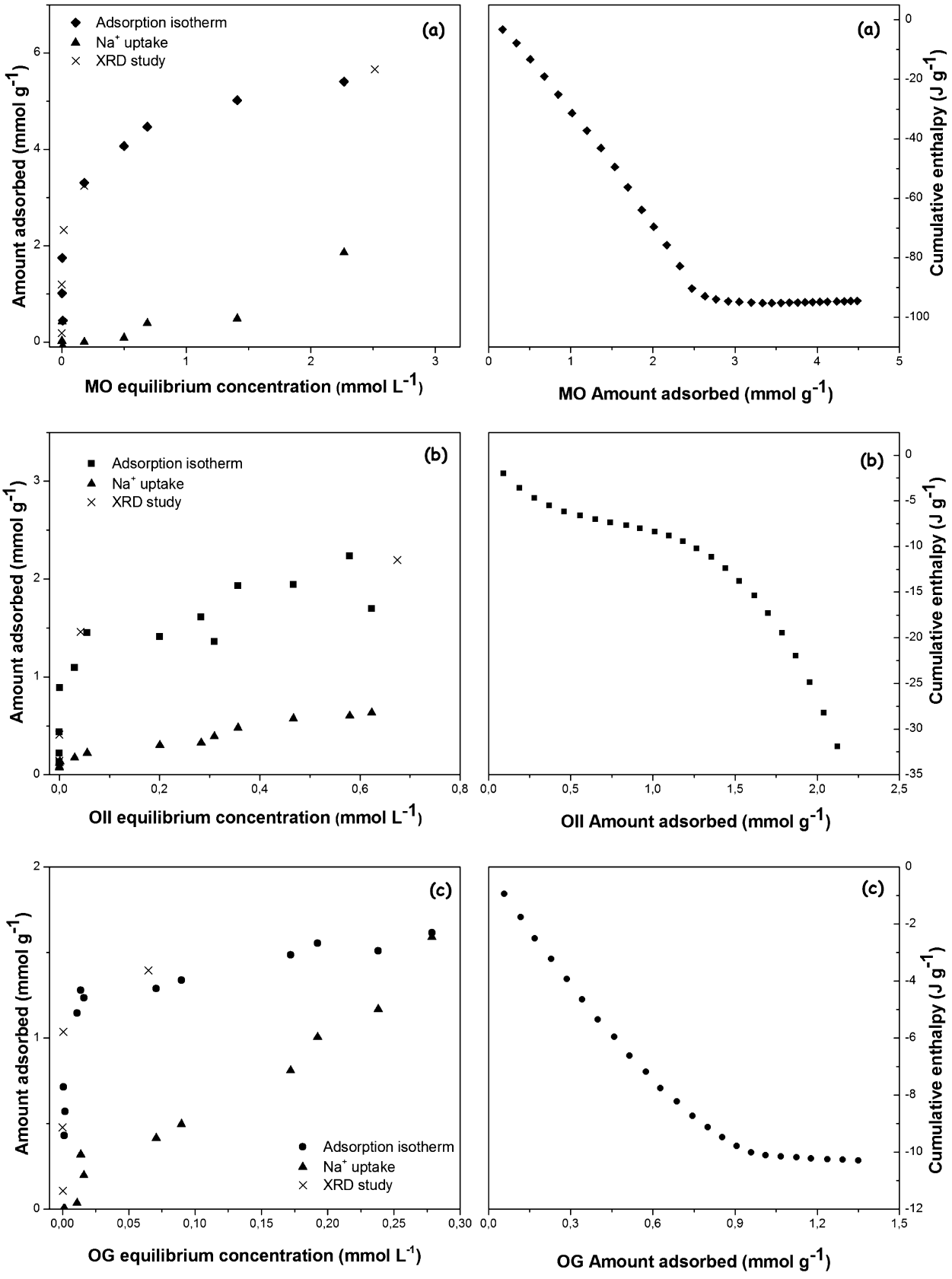

Figure 3. Left panels: adsorption isotherms for MO (a), OII (b), and OG (c) anions and sodium cations from aqueous solutions onto Mg–Al–LDH–NO_3 at 25 °C. Right panels: variations of the cumulative enthalpy of displacement as a function of the amount of dye adsorbed.

MO; 2.7 mmol g^{-1}, OII; 1.7 mmol g^{-1}, OG. The modification of pH during sorption is rather small. For OG and OII, the pH of the suspension does not vary a lot (0.1–0.2 pH unit, OG; 0.2–0.4 pH unit, OII). In the case of MO, the pH change is

DOI: 10.1021/acs.jpcc.5b05510
J. Phys. Chem. C 2015, 119, 23388–23397

somewhat higher, with an increase of pH around 1 unit (between 0.6 and 1.3). The observed differences in the maximum adsorption quantities can be obviously correlated with the cross-sectional area of the dye species which increases in the order: MO < OII < OG (see Figure 1). Furthermore, since one OG anion bears two negative charges, the quantity adsorbed of this molecule should be smaller than those of the two others. The hydrophobic−hydrophilic character of each dye unit is another parameter to be considered when explaining the observed trends in the maximum amounts adsorbed. The MO moiety is more hydrophobic than the OII one since it contains additional terminal methyl groups, whereas the hydrophobic character of the latter is diminished by addition of a hydrophilic OH group.[36] In the case of OG, the presence of two SO_3^- groups, together with the hydrophilic OH substituent, renders this anion the less hydrophobic among the three dyes.[37]

It is worth underlying that the MO amount adsorbed is almost twice that of theoretical AEC as inferred from the chemical formula of the pristine LDH sample (see Table 1). Such an LDH performance has never been shown in the literature. Two hypotheses taken from the previous studies can be considered to rationalize this effect. MO anions may adsorb on the external surface of LDH.[25,38] Another possibility corresponds to the formation of some aggregates inside the LDH interlayer space due to the hydrophobic interactions of chromonic MO species between themselves.[39] In both cases, the excess of negative charge relatively to the AEC has to be neutralized by the uptake of some positively charged species.

The uptake of sodium cations during the adsorption of dye anions is illustrated in Figure 3. Sodium is the counterion with respect to the dye sulfonate moiety $-SO_3^-$. It is clear that Na^+ ions are coadsorbed, especially for high dye uptakes. In the case of MO, the sodium uptake curve may be divided into two parts. In the first part, no adsorption of Na^+ can be observed. It corresponds to the vertical part of the MO adsorption isotherm, where the interaction between MO^- anions and LDH is strong and the formers exchange with the pristine NO_3^- counterions. Since the sulfonate moieties of MO anions compensate successively the positive charge of the brucite-like layer, the sodium co-ions cannot enter the interlamellar domain of the LDH host. The coadsorption of Na^+ ions begins at $Q_{ads} > 4$ mmol g^{-1}, where the amount of MO exceeds the AEC of the pristine LDH sample (3.25 mequiv g^{-1}). The excess of adsorbed MO anions is likely due to hydrophobic interactions resulting in the formation of surface-bound aggregate groups.[36] The free $-SO_3^-$ moieties are thus neutralized by the coadsorbed Na^+ ions.

In contrast, coadsorption of sodium cations parallels the adsorption of OII anions at a constant proportion of 1:3. Therefore, there are some negative species (e.g., carbonate impurities from air and also hydroxyl groups) in the interlayer space of LDH whose charge could be partially neutralized by the coadsorption of Na^+ ions.

The isotherm of sodium uptake accompanying the adsorption of OG anions can be divided into three parts, corresponding, respectively, to zero Na^+ adsorption, partial Na^+ coadsorption, and high Na^+ retention. As in the case of MO adsorption, the first part matches the vertical part of the OG adsorption isotherm. The second part falls in line with the beginning of the saturation plateau region. A plausible explanation is that some OG anions are retained only with one negatively charged center, the second one being neutralized with one sodium counterion. When the dye adsorption reaches its maximum value, one Na^+ ion adsorbs, on average, for one retained OG anion.

The above discussion indicates that the mechanism of dye removal from the aqueous phase by Mg−Al−LDH−NO_3 sample is a complex process passing through various stages involving a variety of species retained at the solid−liquid interface or released to the supernatant solution. The displacement is a commonly used term to designate such a process. Direct calorimetry measurements of the enthalpy changes accompanying the displacement process can shed some light on the interactions involved. The variations of the cumulative enthalpy of displacement are plotted against the amount of dye adsorbed in Figure 3.

Despite some marked differences between the three enthalpy curves, the general conclusion drawn from the calorimetric measurements is that the overall process of displacement has an exothermic character. This observation is at variance with the endothermicity of dye adsorption postulated in the previously published papers[14,15,17] describing the sorption of anionic dyes onto LDHs. It should be emphasized that, contrary to the enthalpy quantities determined previously, the direct calorimetry measurement and further data processing employed here provide estimate of the global heat effect accompanying the sorption process. Indeed, the cumulative enthalpy represents a global effect combining such contributions involved in the sorption phenomenon as the intercalation of the adsorbed species, interlayer anion displacement, swelling of the layers, hydration/dehydration effects and also the displacement of other species (such as Na^+ and OH^-). In the case of MO and OG, the exothermic displacement continues up to the end of the vertical portion of the dye adsorption isotherm; then it levels off quite quickly and the displacement becomes almost athermal. The exothermic effect of displacement accompanying the retention of MO species is much more marked than that of OG adsorption. It decreases to about −90 J g^{-1} in the enthalpy plateau region, contrary to the enthalpy change during OG adsorption which diminishes only to about −10 J g^{-1}. The enthalpy variations for OII do not follow the same trend. The initial decrease to about −10 J g^{-1} at the end of the vertical portion of the OII adsorption isotherms is consistent with the enthalpy curve for OG. After a short "hesitation" interval, a new strongly exothermic contribution to the total enthalpy of displacement becomes noticeable. This trend is difficult to be explained on the basis of the results reported here.

According to the well-documented literature,[3,4,8,10,16−18,26] the intercalation of dye anions into the interlayer space of LDH materials may lead to an expansion of the interlayer distance. The results of a similar XRD study made on the selected LDH samples loaded with different amounts of dye anions are reported below. For each type of dye, the quantities of adsorption are marked with crosses directly on the related adsorption isotherms in Figure 3.

X-ray diffraction patterns of Mg−Al−LDH with increasing MO content are shown in Figure 4. They are compared with XRD patterns of the pristine samples containing carbonate and nitrate anions. For the first point in the adsorption isotherm (system MO-1), where there are 0.2 mmol of MO retained per gram of the pristine LDH sample, a displacement of the (003) peak from a 2θ position of 10°−11.5° can be seen. The interlayer distance thus decreases from 0.89 to 0.77 nm. The latter value is consistent with the Mg−Al−LDH−CO_3 system in which the (003) peak is located at 11.6° with a d_{003} value of

DOI: 10.1021/acs.jpcc.5b05510
J. Phys. Chem. C 2015, 119, 23388−23397

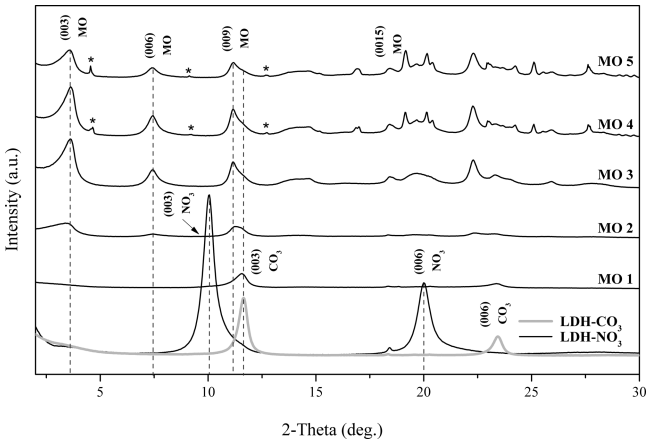

Figure 4. X-ray diffraction patterns in the 2θ range from 2° to 30° for the intercalation of MO in the Mg−Al−LDH−NO_3 structure corresponding to 5 points in the MO adsorption isotherm (as marked by crosses in Figure 3).

0.765 nm. This means that there is no more NO_3 anions within the interlayer space of LDH even for very small MO adsorption quantities. The pristine nitrate anions are thus easily replaced by the carbonate ones, provided by dissolution of CO_2 in water from open system. Moreover, pristine LDHs contain already carbonate species in the structure. The latter phase cannot be observed in the XRD pattern of the pristine material because of the too small carbonate content (Table 1) and because it is masked by the presence of the nitrate phase. However, the displacement of nitrate anions by the incoming MO species makes the CO_3 phase distinguishable in the XRD pattern of the MO-1 system, thought with a very low intensity. It is worth mentioning that there is no important narrowing of the basal spacing in the system with MO^- intercalation, because of the very small quantity adsorbed 0.2 mmol g^{-1}.

In the case of the MO-2 system (Q_{ads} = 1.2 mmol g^{-1}), two new harmonic peaks appear at 2θ positions of 3.6° and 7.4° corresponding to *d*-values of 2.42 and 1.2 nm. These new peaks are ascribed to the (003) and (006) reflections due to MO^- species intercalated in the LDH host. The third (009) harmonic peak should have appeared at 11.1° but it is not clearly distinguishable in Figure 4. Nevertheless, the broadening of the carbonate peak (between 2θ positions from 11.1 to 11.5°) may evidence for the existence of the (009) peak of MO^-. These features in the XRD pattern indicate that MO and CO_3 containing interlayers are present in the LDH.

Further MO uptake (from MO-3 to MO-5) induces an increase of intensity of the (009) reflection with a d value of 0.8 nm. The MO phase becomes predominant already in the MO-3 system. The presence of three (00l) harmonic reflections corresponding to *d*-values of 2.42, 1.2, and 0.8 nm is in good agreement with the previous papers reporting the intercalation patterns in Mg−Al−LDHs,[7,26] Zn−Al−LDHs,[3,13,40] and Ca−Al−LDHs.[13] The expansion of the basal interlayer distance (d_{003}) of the host LDH lattice from 0.89 to 2.42 nm, which parallels the MO intercalation, points toward the successful exchange with NO_3^- anions. Furthermore, three new sharp peaks are visible in the XRD patterns of the MO-4 and MO-5 systems (*). According to the previous discussion, the amounts of MO retained by the LDH host (3.3 and 5.5 mmol g^{-1}, respectively) exceed the AEC of LDH (3.25 mequiv g^{-1}). The possibility of MO sorption or crystallization on the external surface was checked thoroughly by washing, prior to XRD analysis, a LDH sample previously loaded with 3.7 mmol g^{-1} of MO. The resulting diffractogram (not shown here) exhibited only 3 harmonic peaks at 2θ positions of 3.6°, 7.4°, and 11.1°. This corroborated the starting hypothesis of interaction between dye and external surface.

Four different points have been selected in the OII adsorption isotherm (Figure 3b) to perform XRD study on the Mg−Al−LDH−OII systems. The resulting XRD patterns are given in Figure 5. The diffractograms recorded on the

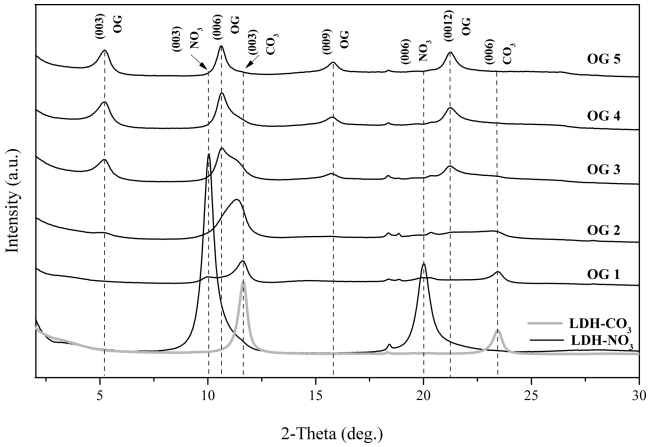

Figure 5. X-ray diffraction patterns in the 2θ range from 2° to 30° for the intercalation of OII in the Mg−Al−LDH−NO_3 structure corresponding to 4 points in the OII adsorption isotherm (as marked by crosses in Figure 3).

pristine LDH−NO_3 and LDH−CO_3 samples are also included for the comparison purpose. The XRD pattern of the OII-1 system (Q_{ads} = 0.14 mmol g^{-1}) exhibits two harmonic peaks at 2θ positions of 11.6° and 23.4°, providing interlayer space distances of 0.76 and 0.38 nm. These (003) and (006) peaks indicate the presence of CO_3^{2-} species in the interlayer space. Moreover, small peaks of the nitrate phase are still present. On the contrary, there are not enough OII units for the peaks of the intercalated species to be distinguishable. With the increased amount of adsorbed OII^- units in the OII-2 system (Q_{ads} = 0.41 mmol g^{-1}), two harmonic (003) and (006) peaks become visible at 2θ positions of 3.9° and 7.9°. These peaks corresponded to interlayer space distances of 2.22 and 1.11 nm and thus indicate the intercalation of OII^- anions within the LDH structure. The (009) harmonic peak of OII has almost the same position as the (003) peak of the intercalated carbonate anions and, therefore, it is difficult to deduce the role of carbonate species during dye intercalation. It is useful to compare the harmonic (006) peak of carbonates with the (0018) peak of OII^- so as to notice the increasing predominance of the OII^- phase when passing from OII-2 to OII-4 system; the (0018) reflection becomes sharper than the (006) peak of carbonates already in the XRD pattern of the OII-3 system. The existence of the CO_3^{2-} phase even in the OII plateau adsorption region confirms the previous hypothesis explaining the coadsorption of sodium cations and OII^- anions at a constant proportion of 1:3. XRD results are in agreement with those reported for OII^- adsorption onto LDH[16,41−43] and LDH-PVA[40] structures. The last unattributed peak could be explained by specific interaction of OII and LDH as observed

DOI: 10.1021/acs.jpcc.5b05510
J. Phys. Chem. C 2015, 119, 23388−23397

from calorimetric results. This mechanism deserves to be studied more in details to check the hypothesis.

Figure 6 shows XRD patterns recorded on LDH samples loaded with increasing amounts of OG units. For the OG-1

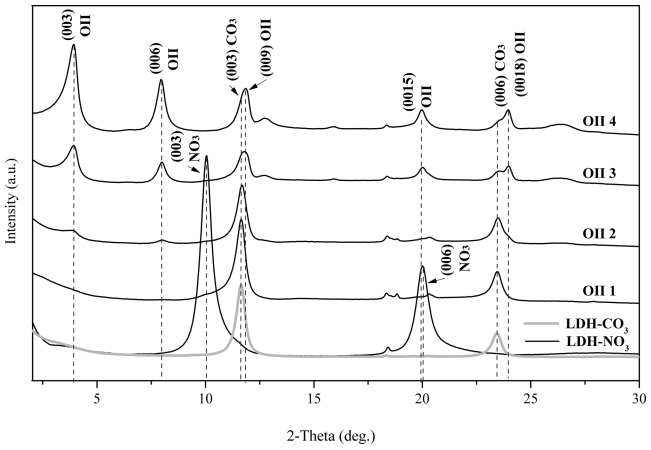

Figure 6. X-ray diffraction patterns in the 2θ range from 2° to 30° for the intercalation of OG in the Mg−Al−LDH−NO_3 structure corresponding to 5 points in the OG adsorption isotherm (as marked by crosses in Figure 3).

system, the corresponding diffractogram clearly indicates the presence of nitrates and carbonates ions in the interlayer space with the related (003) and (003) reflections at 2θ positions of 10° and 11.6°, respectively. The OG phase is not clearly visible probably because of the very small amount adsorbed (about 0.11 mmol g^{-1}). The orientation of the intercalated dye units is likely parallel to the layers and the corresponding peak is hidden by the peaks of CO_3 and NO_3 phases. When one passes to the OG-2 system, a new peak appears at a 2θ position of 5.2°. It can be assigned to the (003) reflection of the OG phase in relation with the interlayer distance of 1.68 nm. Broadening the peaks corresponding, to the (003), (003), and (006) reflections of the NO_3, CO_3 and OG phases respectively can be interpreted as the result of increased adsorption of OG units (Q_{ads} = 0.48 mmol g^{-1}). The NO_3 phase disappears in the XRD pattern recorded on the OG-3 system (Q_{ads} = 1.04 mmol g^{-1}. Simultaneously, the OG phase becomes predominant over the carbonates species, as inferred from the (006) reflection by OG species and the (003) by the CO_3^{2-} ones. Two new harmonic reflections of OG at 2θ positions of 15.8° and 21.1° can be found in the XRD pattern. They may be assigned as the (009) and (0012) reflections of OG species. For the last OG-5 system, no peaks characteristic of the CO_3 phase are visible and the intercalated OG^{2-} species constitute the only phase present in the interlayer space. The expansion of the LDH structure by intercalation of the OG units results in an increase in the interlayer space distance from 0.89 to 1.68 nm. The latter is not far from the 1.77 nm[18] and 1.78 Å[40,44] values reported previously in the literature. Furthermore, this expansion is in a good agreement with the coadsorption of sodium cations and in line with the vertical orientation of the intercalated OG units interacting through only one $-SO_3$ moiety with the positively charged LDH layers.

4. CONCLUSIONS

The combination of various experimental techniques has been applied to study some important aspects of the adsorption of azo anionic dyes from aqueous solutions onto Mg−Al−LDH sample containing nitrate anions in the interlayer space. Despite certain differences in the kinetic behavior among Methyl Orange, Orange II, and Orange G, the adsorption equilibrium is attained after 200 min at the last; the kinetic rate is the highest for OII and the lowest for MO. The dye retention kinetics obeys the pseudo-second-order kinetic model, thereby indicating a strong interaction between the dye units and the LDH host structure. The maximum amount of dye retained in the adsorption plateau region increases in the order: MO ≫ OII > OG. This trend can be first rationalized when taking into account the differences in the molecular sizes, electrical charges, and hydrophobic character of the molecules. In the case of MO, the maximum dye adsorption exceeds the anionic exchange capacity of the pristine LDH material. The retention of the MO units on the external surface and their aggregation inside the interlayer space may be considered to explain this result, which has never been obtained before. The uptake of dye anions by the LDH material can be accompanied by the coadsorption of Na^+ cations and this is a second original contribution of the present study to improve the understanding of the adsorption mechanism. For OII, the Na^+ coadsorption is observed for all points in the adsorption isotherm and, on average, one sodium cation is retained per three OII units. In the case of the two other dyes, the coadsorption of sodium becomes noticeable only for higher dye uptakes. The detailed analysis of XRD patterns recorded on different LDH samples loaded with varying amounts of dye species show that MO, OII, and OG anions are intercalated into the interlayer space of the Mg−Al−LDH−NO_3 structure, thereby displacing nitrate anions to the supernatant aqueous phase. This intercalation step is paralleled by the expansion of the basal interlayer distance (d_{003}) of the host LDH lattice from 0.89 to 2.42 nm, MO; 2.22 nm, OII; 1.68 nm, OG.

In summary, Mg−Al−LDH has been proven to be a good adsorbent for the three Orange-like dyes molecules. The results reported in the present paper indicate the complex mechanism of the adsorption phenomenon involving several species which can either compete against one another for the active sites at the LDH surface or they can give rise to a cooperative adsorption. The overall mechanism is exothermic, especially in the case of MO. This result is at variance with the endothermic character previously reported in the literature on the basis of the modeling studies. Further study on the OII adsorption is necessary to explain the variations of the enthalpy of displacement at higher amounts adsorbed.

■ ASSOCIATED CONTENT

Supporting Information

The Supporting Information is available free of charge on the ACS Publications website at DOI: 10.1021/acs.jpcc.5b05510.

Characteristics of Mg−Al−LDH−NO_3 solid and dye molecules, repeatability and experimental uncertainties, kinetic models (PDF)

■ AUTHOR INFORMATION

Corresponding Author

*Phone: +33 4 67 14 33 05. E-mail: benedicte.prelot@um2.fr.

Notes

The authors declare no competing financial interest.

DOI: 10.1021/acs.jpcc.5b05510
J. Phys. Chem. C 2015, 119, 23388−23397

■ ACKNOWLEDGMENTS

The authors are grateful to Mr. Bernard Fraisse for his assistance with the XRD measurements and to Mr. Amine Geneste for his valuable help with calorimetric experiments.

■ REFERENCES

(1) Verma, A. K.; Dash, R. R.; Bhunia, P. A Review on Chemical Coagulation/Flocculation Technologies for Removal of Colour from Textile Wastewaters. *J. Environ. Manage.* **2012**, *93*, 154−168.
(2) Geethakarthi, A.; Phanikumar, B. R. Industrial Sludge Based Adsorbents/Industrial by-Products in the Removal of Reactive Dyes—A Review. *Int. J. Water Res. Environ. Eng.* **2011**, *3*, 1−9.
(3) Costantino, U.; Coletti, N.; Nocchetti, M.; Aloisi, G. G.; Elisei, F. Anion Exchange of Methyl Orange into Zn-Al Synthetic Hydrotalcite and Photophysical Characterization of the Intercalates Obtained. *Langmuir* **1999**, *15*, 4454−4460.
(4) Ni, Z.-M.; Xia, S.-J.; Wang, L.-G.; Xing, F.-F.; Pan, G.-X. Treatment of Methyl Orange by Calcined Layered Double Hydroxides in Aqueous Solution: Adsorption Property and Kinetic Studies. *J. Colloid Interface Sci.* **2007**, *316*, 284−291.
(5) El Gaini, L.; Lakraimi, M.; Sebbar, E.; Bakasse, M. Removal of Methyl Orange Dye from Water to Zinc-Aluminium-Chloride Layered Double Hydroxides. *J. Optoelectron. Adv. Mater.* **2008**, *10*, 1415−1420.
(6) Mandal, S.; Lerner, D. A.; Marcotte, N.; Tichit, D. Structural Characterization of Azoic Dye Hosted Layered Double Hydroxides. *Zeitschrift für Kristallographie* **2009**, *224*, 282.
(7) Morimoto, K.; Tamura, K.; Iyi, N.; Ye, J.; Yamada, H. Adsorption and Photodegradation Properties of Anionic Dyes by Layered Double Hydroxides. *J. Phys. Chem. Solids* **2011**, *72*, 1037−1045.
(8) Zhang, P.; Wang, T.; Qian, G.; Wu, D.; Frost, R. L. Removal of Methyl Orange from Aqueous Solutions through Adsorption by Calcium Aluminate Hydrates. *J. Colloid Interface Sci.* **2014**, *426*, 44−47.
(9) Zhou, K.; Zhang, Q.; Wang, B.; Liu, J.; Wen, P.; Gui, Z.; Hu, Y. The Integrated Utilization of Typical Clays in Removal of Organic Dyes and Polymer Nanocomposites. *J. Cleaner Prod.* **2014**, *81*, 281−289.
(10) Zhang, P.; Qian, G.; Shi, H.; Ruan, X.; Yang, J.; Frost, R. L. Mechanism of Interaction of Hydrocalumites (Ca/Al-LDH) with Methyl Orange and Acidic Scarlet Gr. *J. Colloid Interface Sci.* **2012**, *365*, 110−116.
(11) Li, Z.; Yang, B.; Zhang, S.; Wang, B.; Xue, B. A Novel Approach to Hierarchical Sphere-Like Znal-Layered Double Hydroxides and Their Enhanced Adsorption Capability. *J. Mater. Chem. A* **2014**, *2*, 10202−10210.
(12) Zheng, Y.-M.; Li, N.; Zhang, W.-D. Preparation of Nanostructured Microspheres of Zn−Mg−Al Layered Double Hydroxides with High Adsorption Property. *Colloids Surf., A* **2012**, *415*, 195−201.
(13) Ai, L.; Zhang, C.; Meng, L. Adsorption of Methyl Orange from Aqueous Solution on Hydrothermal Synthesized Mg−Al Layered Double Hydroxide. *J. Chem. Eng. Data* **2011**, *56*, 4217−4225.
(14) Zaghouane-Boudiaf, H.; Boutahala, M.; Arab, L. Removal of Methyl Orange from Aqueous Solution by Uncalcined and Calcined Mgnial Layered Double Hydroxides (LDHs). *Chem. Eng. J.* **2012**, *187*, 142−149.
(15) Monash, P.; Pugazhenthi, G. Utilization of Calcined Ni-Al Layered Double Hydroxide (LDH) as an Adsorbent for Removal of Methyl Orange Dye from Aqueous Solution. *Environ. Prog. Sustainable Energy* **2014**, *33*, 154−159.
(16) Mustapha Bouhent, M.; Derriche, Z.; Denoyel, R.; Prevot, V.; Forano, C. Thermodynamical and Structural Insights of Orange Ii Adsorption by MgRAlNO$_3$ Layered Double Hydroxides. *J. Solid State Chem.* **2011**, *184*, 1016−1024.
(17) Benselka-Hadj Abdelkader, N.; Bentouami, A.; Derriche, Z.; Bettahar, N.; de Ménorval, L. C. Synthesis and Characterization of Mg−Fe Layer Double Hydroxides and Its Application on Adsorption of Orange G from Aqueous Solution. *Chem. Eng. J.* **2011**, *169*, 231−238.
(18) Extremera, R.; Pavlovic, I.; Pérez, M.; Barriga, C. Removal of Acid Orange 10 by Calcined Mg/Al Layered Double Hydroxides from Water and Recovery of the Adsorbed Dye. *Chem. Eng. J.* **2012**, *213*, 392−400.
(19) Laguna, H.; Loera, S.; Ibarra, I. A.; Lima, E.; Vera, M. A.; Lara, V. Azoic Dyes Hosted on Hydrotalcite-Like Compounds: Non-Toxic Hybrid Pigments. *Microporous Mesoporous Mater.* **2007**, *98*, 234−241.
(20) Gil, A.; Assis, F. C. C.; Albeniz, S.; Korili, S. A. Removal of Dyes from Wastewaters by Adsorption on Pillared Clays. *Chem. Eng. J.* **2011**, *168*, 1032−1040.
(21) Lee, S. M.; Tiwari, D. Organo and Inorgano-Organo-Modified Clays in the Remediation of Aqueous Solutions: An Overview. *Appl. Clay Sci.* **2012**, *59*−*60*, 84−102.
(22) Rives, V.; Angeles Ulibarri, M. a. Layered Double Hydroxides (Ldh) Intercalated with Metal Coordination Compounds and Oxometalates. *Coord. Chem. Rev.* **1999**, *181*, 61−120.
(23) Sato, T.; Fujita, H.; Endo, T.; Shimada, M.; Tsunashima, A. Synthesis of Hydrotalcite-Like Compounds and Their Physico-Chemical Properties. *React. Solids* **1988**, *5*, 219−228.
(24) Elmoubarki, R.; Mahjoubi, F. Z.; Tounsadi, H.; Moustadraf, J.; Abdennouri, M.; Zouhri, A.; El Albani, A.; Barka, N. Adsorption of Textile Dyes on Raw and Decanted Moroccan Clays: Kinetics, Equilibrium and Thermodynamics. *Water Resources and Industry* **2015**, *9*, 16−29.
(25) Rives, V. *Layered Double Hydroxides: Present and Future*; Nova Publishers: Hauppauge, NY, 2001.
(26) Mandal, S.; Tichit, D.; Lerner, D. A.; Marcotte, N. Azoic Dye Hosted in Layered Double Hydroxide: Physicochemical Characterization of the Intercalated Materials. *Langmuir* **2009**, *25*, 10980−10986.
(27) Ay, A. N.; Zumreoglu-Karan, B.; Mafra, L. A Simple Mechanochemical Route to Layered Double Hydroxides: Synthesis of Hydrotalcite-Like Mg-Al-NO$_3$-LDH by Manual Grinding in a Mortar. *Z. Anorg. Allg. Chem.* **2009**, *635*, 1470−1475.
(28) Lagergren, S. Zur Theorie Der Sogenannten Adsorption Gelöster Stoffe: Kungliga Svenska Vetenskapsakademiens; Handlingar, 1898.
(29) Ho, Y.-S.; McKay, G. Pseudo-Second Order Model for Sorption Processes. *Process Biochem.* **1999**, *34*, 451−465.
(30) Ho, Y.-S.; McKay, G. Kinetic Models for the Sorption of Dye from Aqueous Solution by Wood. *Process Saf. Environ. Prot.* **1998**, *76*, 183−191.
(31) Prelot, B.; Ayed, I.; Marchandeau, F.; Zajac, J. On the Real Performance of Cation Exchange Resins in Wastewater Treatment under Conditions of Cation Competition: The Case of Heavy Metal Pollution. *Environ. Sci. Pollut. Res.* **2014**, *21*, 9334−9343.
(32) Chen, H.; Dai, G.; Zhao, J.; Zhong, A.; Wu, J.; Yan, H. Removal of Copper(II) Ions by a Biosorbent-Cinnamomum Camphora Leaves Powder. *J. Hazard. Mater.* **2010**, *177*, 228−236.
(33) Arami, M.; Limaee, N. Y.; Mahmoodi, N. M. Evaluation of the Adsorption Kinetics and Equilibrium for the Potential Removal of Acid Dyes Using a Biosorbent. *Chem. Eng. J.* **2008**, *139*, 2−10.
(34) Poots, V. J. P.; McKay, G.; Healy, J. J. Removal of Basic Dye from Effluent Using Wood as an Adsorbent. *J. - Water Pollut. Control Fed.* **1978**, 926−935.
(35) Giles, C. H.; MacEwan, T.; Nakhwa, S.; Smith, D. Studies in Adsorption. Part Xi. A System of Classification of Solution Adsorption Isotherms, and Its Use in Diagnosis of Adsorption Mechanisms and in Measurement of Specific Surface Areas of Solids. *J. Chem. Soc.* **1960**, 3973−3993.
(36) Reeves, R. L.; Harkaway, S. A. Surface Tensions of Aqueous Solutions of Some Azo Dye Sulfonates and Analogs. *J. Colloid Interface Sci.* **1978**, *64*, 342−347.
(37) Madhavan, J.; Grieser, F.; Ashokkumar, M. Degradation of Orange-G by Advanced Oxidation Processes. *Ultrason. Sonochem.* **2010**, *17*, 338−343.
(38) Châtelet, L.; Bottero, J. Y.; Yvon, J.; Bouchelaghem, A. Competition between Monovalent and Divalent Anions for Calcined

DOI: 10.1021/acs.jpcc.5b05510
J. Phys. Chem. C 2015, 119, 23388−23397

and Uncalcined Hydrotalcite: Anion Exchange and Adsorption Sites. *Colloids Surf., A* **1996**, *111*, 167−175.
(39) Lydon, J. Chromonic Liquid Crystal Phases. *Curr. Opin. Colloid Interface Sci.* **1998**, *3*, 458−466.
(40) Marangoni, R.; da Costa Gardolinski, J. E. F.; Mikowski, A.; Wypych, F. Pva Nanocomposites Reinforced with ZN_2Al LDHs, Intercalated with Orange Dyes. *J. Solid State Electrochem.* **2011**, *15*, 303−311.
(41) Géraud, E.; Bouhent, M.; Derriche, Z.; Leroux, F.; Prévot, V.; Forano, C. Texture Effect of Layered Double Hydroxides on Chemisorption of Orange Ii. *J. Phys. Chem. Solids* **2007**, *68*, 818−823.
(42) Liu, L.-Y.; Pu, M.; Yang, L.; Li, D.-Q.; Evans, D. G.; He, J. Experimental and Theoretical Study on the Structure of Acid Orange 7-Pillared Layered Double Hydroxide. *Mater. Chem. Phys.* **2007**, *106*, 422−427.
(43) Melánová, K.; Beneš, L.; Zima, V.; Svoboda, J. Intercalation of Dyes Containing SO_3H Groups into Zn−Al Layered Double Hydroxide. *J. Inclusion Phenom. Mol. Recognit. Chem.* **2005**, *51*, 97−101.
(44) Marangoni, R.; Ramos, L. P.; Wypych, F. New Multifunctional Materials Obtained by the Intercalation of Anionic Dyes into Layered Zinc Hydroxide Nitrate Followed by Dispersion into Poly (Vinyl Alcohol) (Pva). *J. Colloid Interface Sci.* **2009**, *330*, 303−309.

DOI: 10.1021/acs.jpcc.5b05510
J. Phys. Chem. C 2015, 119, 23388−23397